Modelling of a Single Degree of Freedom Flexible Arm Pneumatically Operated

Fernando F. Kiyama and Emilio Vargas

Abstract— This paper is about the modelling of one of the degrees of freedom of an industrial flexible manipulator, pneumatically operated by means of a cushion type air cylinder. Pneumatic modelling is made upon the thermodynamic principles of mass and energy conservation, the flexible arm model is made using constrained generalized coordinates, and the assumed modes method. A manipulator prototype was built and instrumented, its experimental data is presented for model verification purposes. The flexible arm simulated vibration is compared both, with the results obtained upon the identification of the arm generalized coordinates and direct vibration measurements.

Index Terms— pneumatic cylinder, flexible manipulator, modelling, robotics, assumed modes.

I. INTRODUCTION

TRADITIONALLY the structural rigidity of robots has been a fundamental characteristic to achieve speed and accuracy. This rigidity means more weight and inertia, requiring an increase in the size of the actuators and more power to operate at the same speed. With the development of robots with high speed, high precision and heavy load, the effect of elastic deformation must be taken into consideration.

Some particular systems, such as light industrial manipulators and the large space structures require lightweight elements. Weight reduction however, results in lack of sensing, vibration, and incapability of precise positioning because of the flexibility of the system, and difficulty to obtain accurate model.

Flexible manipulator modelling, has been done for many years to describe its dynamic behavior and improving it. Several methods have been proposed to consider the effect of elasticity. One is the assumed modes method, which presupposes the displacement function to establish the movement equation [1], [2], [3]. Another is the finite element method, which divides the link into discrete elements to derive the system equations [4], [5]. A third method commonly adopted by many researchers, is the lumped parameter method, similar to the finite element method but reducing the amount of calculation [6], [7].

Since modelling of flexible manipulators is very complex, many researches consider as a first step only one link as

F. Kiyama is with the Centro Regional de Optimización y Desarrollo de Equipo, Homero 350, Complejo Industrial Chihuahua, Chihuahua, Chih. C.P. 31109, e-mail fkiyamam@yahoo.com.mx

E. Vargas is with the Centro de Ingeniería y Desarrollo Industrial, Playa Pie de la Cuesta 702, Col. Desarrollo San Pablo, Querétaro, Qro. C.P. 76130, e-mail emilio@mecatronica.net
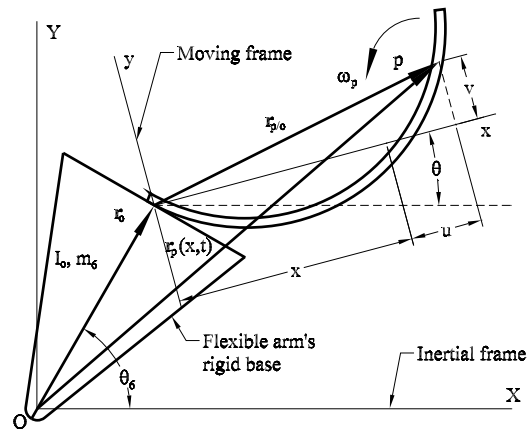

Fig. 1. Arm deformation about inertial coordinates

flexible [7], [5]. Nevertheless powerful computers have enabled to consider several links to be flexible [1], [2], [3], [4], [6].

This paper presents the modelling of one degree of freedom, for an industrial type flexible manipulator, operated by a pneumatic cylinder equipped with break cushions. The elasticity of the arm is modelled using constrained generalized coordinates and the assumed modes method. The description of the dynamics of the control valve and the linear actuator is presented, and the considerations to model the system friction force effects are proposed, as a variation of the Van de Vrande smooth function [15]. Simulation results are presented and compared with experimental data for validation purposes.

This work is part of the development on an industrial dielectric manipulator, designed for the cleaning maintenance of insulators in electric power lines, [8].

II. DYNAMIC MODEL OF THE MANIPULATOR

The arm structure consists of a rigid base and a flexible bar, which actually is a two link chain as shown in Figure 1, operating in the vertical plane. The rigid base is pivoted in the origin of the inertial frame XY, the flexible bar is fixed to the rigid base, and attached to a moving reference frame xy.

II-A. Kinematics and Dynamics of the Mechanism

The kinematics of the flexible arm is defined as shown in Figure 1 by the parametric representation of the beam shape,

namely the vectorial function r_p considered for a point p upon the transversal section of the arm:

$$\boldsymbol{r_p}(x,t) = \boldsymbol{r_0}(t) + (x + u(x,t))\,\boldsymbol{i} + v(x,t)\boldsymbol{j} \qquad (1)$$

The elastic displacement profile is described by a finite sum of assumed modes:

$$v = \sum_{r=1}^{n} \psi_r(x)q_r(t) \qquad (2)$$

$\psi_r(x)$ are spatially-dependent assumed modes, $q_r(t)$ are time-dependent generalized coordinates and n is the number of modes.

From 1 the kinetic energy can be written as:

$$T = \frac{1}{2}I_6\dot{\theta_6}^2 + \frac{1}{2}\int_0^L \mu \boldsymbol{r_p}(x,t) \cdot \boldsymbol{r_p}(x,t)dx \qquad (3)$$

where I_6 is the mass inertial moment of the rigid base about the inertial frame, μ is the mass of the arm per unit length and L is the length of the arm. The first term in 3, gives the kinetic energy of the rigid base, and the second term considers only the translational kinetic energy of the arm, because the rotational energy is very small.

Considering that the arm deforms in the XY plane only, the potential energy will be given by:

$$V = \frac{1}{2}\int_0^L EI\,(v"(x,t))^2\,dx \qquad (4)$$

where EI is the bending stiffness of the arm. The model is simplified by ignoring the axial deformation for being small.

The effect of gravity and of applied forces can be considered from virtual work:

$$\delta W = \boldsymbol{F_{56}} \cdot \delta \boldsymbol{r_{15}} - m_6 \boldsymbol{g_0} \cdot \delta \boldsymbol{r_{6G}} - \int_0^L \mu \boldsymbol{g_0} \cdot \delta \boldsymbol{r_p}\,dx \qquad (5)$$

where $\boldsymbol{F_{56}}$ is the driving force, $\delta \boldsymbol{r_{15}}$ is the virtual displacement of the point of application of the driving force, m_6 is the mass of the rigid base, $\boldsymbol{g_0}$ is the gravitational acceleration and $\delta \boldsymbol{r_{6G}}$ is the virtual displacement of the mass center of the rigid base.

By substituting equations 1, 2, 3, 4 and 5 into Lagrange's equations, the equations of motion are obtained. They are given by the following:

$$(\mu Lr_0^2 + I_6)\ddot{\theta}_6 + \frac{1}{2}\left(\mu L^2 r_0 - \{q\}^T[J]\{q\}\right)\ddot{\theta}cos(\theta - \theta_6)$$
$$-\{b\}^T\{q\}\ddot{\theta}sin(\theta - \theta_6) + \{b\}^T\{\ddot{q}\}cos(\theta - \theta_6)$$
$$-2\{b\}^T\{\dot{q}\}\dot{\theta}sin(\theta - \theta_6)$$
$$-(\{b\}^T\{q\}\dot{\theta} + \{q\}^T[J]\{\dot{q}\})\dot{\theta}cos(\theta - \theta_6)$$
$$-\frac{1}{2}(\mu L^2 r0 - \{q\}^T[J]\{q\})\dot{\theta}^2 sin(\theta - \theta_6)$$
$$= (\mu Lr_0 + m_6 r_{6G})g_0 sin\theta_6$$
$$+ r_{15}(F_{56y}cos\theta_6 - F_{56x}sin\theta_6) \qquad (6)$$
$$\frac{1}{2}(\mu L^2 r_0 - \{q\}^T[J]q)\ddot{\theta}_6 cos(\theta - \theta_6)$$
$$-\{b\}^T\{q\}\ddot{\theta}_6 sin(\theta - \theta_6) + \{q\}^T([M] - [H])\{q\}\ddot{\theta}$$

$$+I_0\ddot{\theta} + \{a\}^T\{\ddot{q}\} + 2\{q\}^T([M] - [H])\{\dot{q}\}\dot{\theta}$$
$$+(\{b\}^T\{q\}\dot{\theta}_6 - \{q\}^T[J]\{\dot{q}\})\dot{\theta}_6 cos(\theta - \theta_6)$$
$$+\frac{1}{2}(\mu L^2 r_0 - \{q\}^T[J]\{q\})\dot{\theta}_6^2 sin(\theta - \theta_6)$$
$$= \frac{1}{2}(\mu g_0 L^2 - \{q\}^T[G]\{q\})sin\theta + \{q\}^T\{g\}cos\theta \qquad (7)$$

$$\{b\}\ddot{\theta}_6 cos(\theta - \theta_6) + \{a\}\ddot{\theta} + [M]\{\ddot{q}\} + \{b\}\dot{\theta}_6^2 sin(\theta - \theta_6)$$
$$-([M] - [H])\{q\}\dot{\theta}^2 + [J]\{q\}\dot{\theta}_6\dot{\theta}cos(\theta - \theta_6) + [K]\{q\}$$
$$= [G]\{q\}cos\theta + \{g\}sin\theta \qquad (8)$$

where I_0 is the "rigid" mass moment of inertia of the flexible arm about the origin of the moving frame. The matrix coefficients in 6, 7 and 8 are defined in terms of the assumed modes as shown below:

$$J_{r,s} = \int_0^L \mu r_0 \int_0^x \psi_r'(\sigma)\psi_s'(\sigma)d\sigma dx \qquad (9)$$

$$b_r = \int_0^L \mu r_0 \psi_r(x)dx \qquad (10)$$

$$M_{r,s} = \int_0^L \mu \psi_r(x)\psi_s(x)dx \qquad (11)$$

$$H_{r,s} = \int_0^L \mu x \int_0^x \psi_r'(\sigma)\psi_s'(\sigma)d\sigma dx \qquad (12)$$

$$a_r = \int_0^L x\mu\psi_r(x)dx \qquad (13)$$

$$G_{r,s} = \int_0^L \mu g_0 \int_0^x \psi_r'(\sigma)\psi_s'(\sigma)d\sigma dx \qquad (14)$$

$$g_r = \int_0^L \mu g_0 \psi_r(x)dx \qquad (15)$$

$$K_{r,s} = \int_0^L EI_z\psi_r"(x)\psi_s"(x)dx \qquad (16)$$

equations 6 and 7 describe the movements of the rigid base and the moving frame respectively, whereas 8 is a set of n equations describing the elastic movement of the arm.

II-B. The Assumed Modes

The use of the moving frame to describe the motion of the manipulator, introduces the additional variable θ (see Figure 1), which requires an additional constraint equation to deal with. The constraint determines the boundary conditions associated with the elastic movement. The adequate selection of assumed modes guarantees the constraint to be satisfied, being equal to choose a set of independent generalized coordinates.

Considering that the rigid base and the flexible arm form an unarticulated unit, it would be natural to consider the zero slope constraint, therefore selecting assumed modes such that the elastic movement has zero slope in the arm's attachment to the base, this allows to express the angular position θ of the moving frame in terms of the angular position θ_6 of the rigid base, rendering simpler equations of motion, unfortunately in this work it was found in practice as [9] indicates, that this constraint leads to an inaccurate model. The inaccuracy is related with the $([M] - [H])$ term in the equations of motion

as explained in [10].

In the model proposed the rigid body constraint is used, which forces the secondary motion to have no rigid body components. The constraint has the form:

$$\frac{1}{\sqrt{I_0}} \int_0^L \mu x v(x,t) dx = 0 \tag{17}$$

II-C. Differential-Algebraic Formulation

The model of the flexible manipulator as considered in the previous section represents a two link pined chain, so we introduce a constraint equation to express the perpendicularity between the rigid base position, and the slope of the flexible arm's attachment:

$$\boldsymbol{f}(\boldsymbol{q}) = \left[\frac{\partial \boldsymbol{r_p}}{\partial x}\right]_{x=0} + \frac{1}{\|\boldsymbol{r_0}\|} \frac{\partial \boldsymbol{r_0}}{\partial \theta_6} = 0 \tag{18}$$

Gathering equations 6, 7 and 8 together with 18 becomes the differential-algebraic system shown below:

$$\dot{\boldsymbol{q}} = \boldsymbol{z} \tag{19}$$

$$\boldsymbol{M}(\boldsymbol{q})\dot{\boldsymbol{z}} = \boldsymbol{h}(\boldsymbol{q},\boldsymbol{z}) - \boldsymbol{F}^T(\boldsymbol{q})\lambda_1 \tag{20}$$

$$0 = \boldsymbol{f}(\boldsymbol{q}) \tag{21}$$

where $\boldsymbol{M}(\boldsymbol{q})$ is the "mass" matrix, $\boldsymbol{F}(\boldsymbol{q}) = \partial \boldsymbol{f}/\partial \boldsymbol{q}$, $\boldsymbol{q} = \{\theta_6, \theta, q_1, \ldots, q_n\}^T$, $\boldsymbol{z} = \{\dot{\theta}_6, \dot{\theta}, \dot{q}_1, \ldots, \dot{q}_n\}^T$ and λ_1 is the Lagrange multiplier.

Integrating numerically the equations 19, 20 and 21 the error in satisfying the constraint grows with time. For this reason the Gear, Gupta & Leimkuhler [11] formulation is used, that involves adding the constraint 18 in velocity form, therefore introducing an additional Lagrange multiplier λ_2 in equation 19, and for symmetry multiplying it by $\boldsymbol{M}(\boldsymbol{q})$, so that the whole system becomes:

$$\boldsymbol{M}(\boldsymbol{q})\dot{\boldsymbol{q}} = \boldsymbol{M}(\boldsymbol{q})\boldsymbol{z} - \boldsymbol{F}^T(\boldsymbol{q})\lambda_2 \tag{22}$$

$$\boldsymbol{M}(\boldsymbol{q})\dot{\boldsymbol{z}} = \boldsymbol{h}(\boldsymbol{q},\boldsymbol{z}) - \boldsymbol{F}^T(\boldsymbol{q})\lambda_1 \tag{23}$$

$$0 = \boldsymbol{f}(\boldsymbol{q}) \tag{24}$$

$$0 = \boldsymbol{F}(\boldsymbol{q})\boldsymbol{z} \tag{25}$$

this formulation keeps the constraint error along the integration within reasonable limits. The λ_1 term in equation 23, calculates the necessary torque at the fixed end of the arm to satisfy the constraint 24, while the λ_2 term in equation 22, corrects the velocity to maintain the constraint error at minimum.

II-D. Pneumatic Modelling

The manipulator is driven by a single-rod pneumatic cylinder, equipped with brake cushions to limit the speed of the piston, that could damage itself when it bumps the cylinder extremities. The pneumatic modelling comprises the flow model through the control valve, and the pneumatic pressure model within the cylinder chambers. Our analysis is similar to the one proposed by [12] and [13], but we extended it to model the behavior of the brake cushioned actuator. The
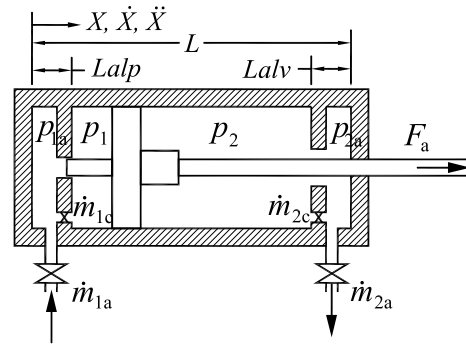

Fig. 2. Pneumatic actuator with cushion chambers

reader is referred to [14] for the details on intermediate steps of derivation. Throughout the pneumatic analysis the following assumptions are used:

A1   Gas is ideal.
A2   Gas density is uniform in the chambers.
A3   Flow in the control valves is isentropic.
A4   Gas in the chambers are isothermal processes.

II-D.1. Flow dynamics through the control valve: The mass flow rate $\dot{m}$ can be described as a function of the valve opening A_t, and the state properties of the gas. A converging nozzle is a good model for the valve. From the continuity equation:

$$\dot{m} = \rho_t A_t v_t \tag{26}$$

where ρ_t and v_t are the density and velocity of the gas in the valve's throat. The mass flow rate can be obtained, depending on the values of the inlet valve pressure p_0, and outlet valve pressure p_1:

$$\dot{m} = C_d \gamma \sqrt{\frac{k}{RT_0}} p_0 A_t \tag{27}$$

$$\gamma = \sqrt{\frac{2}{k-1}} \left(\frac{p_t}{p_0}\right)^{\frac{1+k}{2k}} \left[\left(\frac{p_t}{p_0}\right)^{\frac{1-k}{k}} - 1\right]^{\frac{1}{2}} \tag{28}$$

where k and R are the ratio of specific heats c_p/c_v, and the gas constant respectively, T_0 is the inlet temperature, p_t is the throat pressure, and C_d is the discharge coefficient.

The flow pattern in the valve depends on the values of the pressures p_0 and p_1. For $(1 \geq \frac{p_1}{p_0} \geq 0{,}528)$ the flow is described by equation 28, it varies from $\gamma = 0$ where the actuator's piston does not move and there is no flow through the valve, to $\gamma = 0{,}5787$ where the flow reaches its critical regime. At this point, the velocity of the gas in the throat is equal to the speed of sound calculated at the throat, and would not get larger even if the pressure difference increases, therefore further reducing the outlet pressure p_1 will not affect the flowing state at the throat, in this regime the pressure of the jet leaving the throat p_t is greater than the outlet pressure p_1.

II-D.2. Dynamic relationship within the actuator chambers: The pneumatic actuator is a double-acting linear air cylinder as shown in figure 2. Considering a control volume

that comprises one chamber of the cylinder, the first law of thermodynamics can be written as:

$$\dot{Q} + \dot{m}\left(h + \frac{v^2}{2}\right) = \frac{\partial E}{\partial t} + \dot{W} \tag{29}$$

where $\dot{Q}$ is the heat rate to the control volume and is considered small, the energy of the mass flow rate $\dot{m}$, is given by the enthalpy h of the gas stream through the frontier of the control volume, and its kinetic energy, $\partial E/\partial t$ is the rate of change of energy of the control volume, and $\dot{W}$ is the work rate done on the actuator's piston.

The energy of the mass flow rate $\dot{m}$, can be associated with the stagnation enthalpy:

$$h_0 = c_p T_0 = \left(h + \frac{v^2}{2}\right) \tag{30}$$

The rate of change of energy of the control volume, is mainly given by the rate of change of its internal energy :

$$\frac{\partial E}{\partial t} = \frac{\partial U}{\partial t} = \frac{c_v}{R}\left(\dot{p}V + p\dot{V}\right) \tag{31}$$

where p and V are the pressure and volume inside the chamber. The work rate done by the gas is:

$$\dot{W} = p\dot{V} \tag{32}$$

Taking the origin $(X = 0)$ to be the far left end of the cylinder, and the piston stroke length as L (see figure 2), the chamber volumes are:

$$V_1 = A_p(X + \Delta) \tag{33}$$
$$V_2 = (A_p - A_r)(L - X + \Delta) \tag{34}$$

where V_1 and V_2 are the chamber volumes at the piston and rod sides respectively, A_p and A_r are the piston areas at the "piston" and "rod" sides respectively and Δ is an equivalent extra length of the cylinder to account for the residual volume generated by the connecting tubes and components.

Substituting equations 30, 31, 32, 33 and 34 into equation 29, and simplifying terms, results the next two equations for the chambers at each side of the piston:

$$\dot{m}_1 = \frac{A_p}{kRT_0}\dot{p}_1(X + \Delta) + \frac{A_p}{RT_0}p_1\dot{X} \tag{35}$$
$$\dot{m}_2 = \frac{A_p - A_r}{kRT_0}\dot{p}_2(L - X + \Delta) - \frac{A_p - A_r}{RT_0}p_2\dot{X} \tag{36}$$

Depending on the piston position, the rate of change of pressure inside the cylinder chambers, including the cushions as shown in figure 2, can be calculated from equations 35 and 36:

If $0 \le X \le Lalp$ then

$$\dot{p}_{1a} = \frac{kRT_0}{A_{ap}\left(X + \frac{\Delta A_p}{A_{ap}}\right)}\left[\dot{m}_{1a} - \dot{m}_{1c} - \frac{A_{ap}}{RT_0}p_{1a}\dot{X}\right] \tag{37}$$

$$\dot{p}_1 = \frac{kRT_0}{(A_p - A_{ap})X}\left[\dot{m}_{1c} - \frac{A_p - A_{ap}}{RT_0}p_1\dot{X}\right] \tag{38}$$
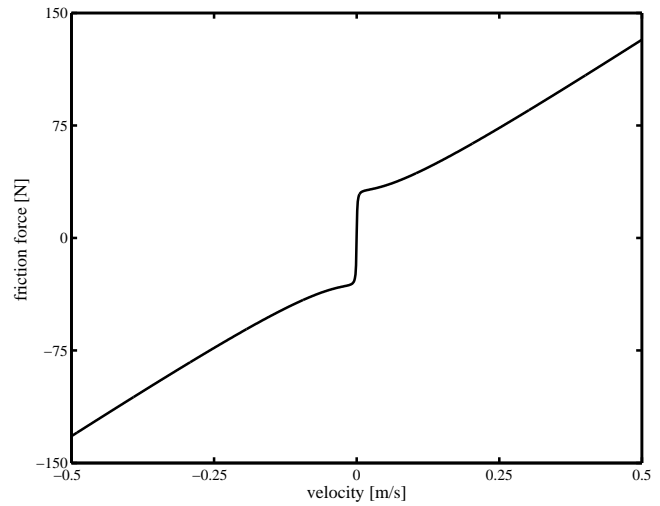

Fig. 3. Piston friction force as a function of relative velocity

If $Lalp < X \le L$ then

$$\dot{p}_{1a} = \frac{kRT_0}{A_p(X + \Delta)}\left[\dot{m}_{1a} - \frac{A_p}{RT_0}p_{1a}\dot{X}\right] \tag{39}$$

$$\dot{p}_1 = \frac{kRT_0}{A_p(X + \Delta)}\left[\dot{m}_{1c} - \frac{A_p}{RT_0}p_1\dot{X}\right] \tag{40}$$

If $0 \le X < (L - Lalv)$ then

$$\dot{p}_2 = \frac{kRT_0}{(A_p - A_r)(L - X + \Delta)} \\ \left[\dot{m}_{2c} + \frac{A_p - A_r}{RT_0}p_2\dot{X}\right] \tag{41}$$

$$\dot{p}_{2a} = \frac{kRT_0}{(A_p - A_r)(L - X + \Delta)} \\ \left[\dot{m}_{2a} + \frac{A_p - A_r}{RT_0}p_{2a}\dot{X}\right] \tag{42}$$

If $(L - Lalv) \le X \le L$ then

$$\dot{p}_2 = \frac{kRT_0}{(A_p - A_r)(L - X)}\left[\dot{m}_{2c} + \frac{A_p - A_r}{RT_0}p_2\dot{X}\right] \tag{43}$$

$$\dot{p}_{2a} = \frac{kRT_0}{L - X + \frac{\Delta A_p}{A_{av} - A_v}}\left[\frac{\dot{m}_{2a} - \dot{m}_{2c}}{A_{av} - A_r} + \frac{p_{2a}\dot{X}}{RT_0}\right] \tag{44}$$

the set of equations from 37 to 44 describe the pressure variation within the actuator chambers.

II-D.3. Friction Forces Model: The friction effect on the seals of the actuator piston is important and should be taken in account. The model proposed is a variation of the friction curve approximated by a smooth function [15]:

$$F_{dv} = K_v\dot{X} + K_c sgn(\dot{X}) + \frac{\alpha sgn(\dot{X}) + K_s(\frac{2}{\pi})tan^{-1}(\beta\dot{X})}{1 + \delta|\dot{X}|} \tag{45}$$

equation 45 gathers the effects of static friction K_s, Stribeck effect given by the last term of equation 45, Coulomb friction K_c and viscous friction K_v.
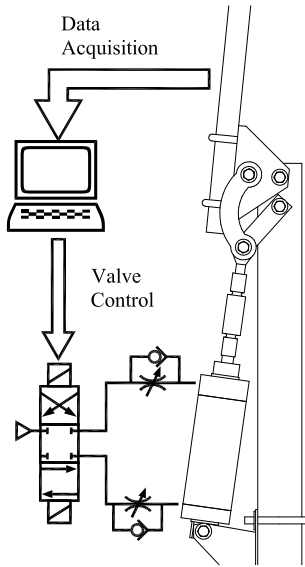
Fig. 4. Experimental arrangement of the flexible manipulator

Fig. 5. Vibration as measured with an accelerometer and strain gages

Figure 3 shows values of the total friction force F_{dv} depending on the relative piston velocity $\dot{X}$ for $K_v = 250N - s/m$, $K_c = 2N$ y $K_s = 30N$. The form coefficients values are $\alpha = 1$, $\beta = 10^3$ and $\delta = 10$.

The force delivered by the cylinder rod, depends on the pressure difference between piston sides, and the the total friction force:

$$F_a = p_1 A_p - p_2(A_p - A_r) - F_{dv} \qquad (46)$$

II-E.   Driving Mechanism Dynamics

The manipulator arm is air pressure driven, by means of a kinematic chain formed by the pneumatic cylinder, as a slider-crank mechanism pinned to a four bar mechanism, as shown in figure 4. The dynamic description of the driving mechanism results from the Newton-Euler formulation:

$$\frac{\mathrm{d}}{\mathrm{d}t}\boldsymbol{p}_i = \boldsymbol{F}_i$$

$$\frac{\mathrm{d}}{\mathrm{d}t}\boldsymbol{H}_{Gi} = \boldsymbol{M}_{Gi} \quad i = 2, 3, \ldots, 6 \qquad (47)$$

where $\boldsymbol{p}_i$ and $\boldsymbol{H}_{Gi}$ are for the link i its linear and angular momentum respectively, $\boldsymbol{F}_i$ and $\boldsymbol{M}_{Gi}$ are the sum of forces and moments acting over the link i. The usage of 47 requires the previous position and velocity analysis of the whole mechanism, for this purpose, the Professor F. H. Raven vectorial approach is used as described in [16]. To solve 47, the input variable is 46 and the output variables are the contact forces between links, and their accelerations that can be written as functions of the piston acceleration $\ddot{X}$.

III.   MODEL VALIDATION

In order to ascertain the validity of the model response, it is necessary to compare it with experimental data, therefore a test prototype was built and instrumented.
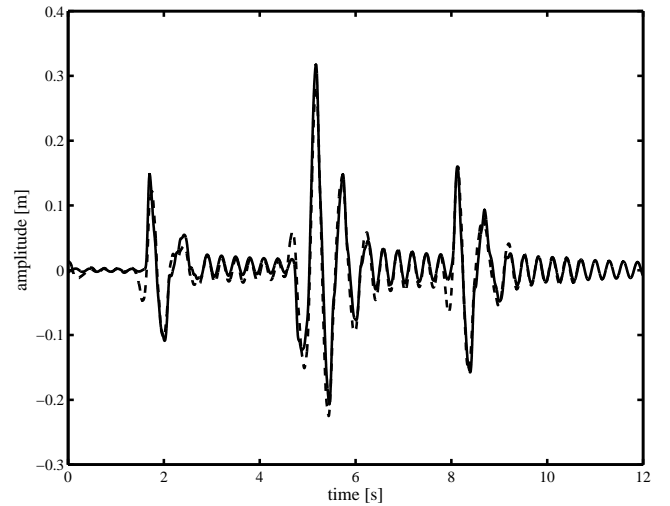
III-A.   Physical description of the Prototype

The flexible arm is a $27mm$ PVC pipe, $1,5m$ long, attached to a rigid base. The arm base is linked to the pneumatic cylinder, by means of a rigid four bar mechanism as shown in figure 4.

The actuator is a double action cylinder, $64mm$ in diameter and $102mm$ stroke. The air flow is regulated by two free return needle valves and the air direction is controlled with a three position, closed center directional valve, the timed opening and closing sequence of this valve is preprogrammed in LabView, where several key variables are also recorded.

The instrumentation considered to measure the prototype response is as follows: pressure sensors for each of the two cylinder ports, a load cell attached to the piston rod, and a potentiometer to record the flexible arm base position. The arm vibration is measured, with an accelerometer attached to the free end of the flexible arm, and also using eight pairs of strain gages glued along the arm.

III-B.   Generalized coordinates identification

The elastic displacement profile of the flexible arm is described by equation 2, therefore the flexure stretch of a point away from the beam axis is $s = h\mathrm{d}v/\mathrm{d}x$, where h is the perpendicular distance from the neutral axis. The strain in the x direction is:

$$\varepsilon = h\frac{\mathrm{d}^2 v}{\mathrm{d}x^2} = \sum_{r=1}^{n} \psi"_r(x)q_r(t) \qquad (48)$$

From data collected with the strain gages and equation 48, the identification of the generalized coordinates was accomplished, and the vibration of the arms free end modelled using equation 2. This vibration is depicted using continuous line and compared with the accelerometer measurements in dashed lines in figure 5.
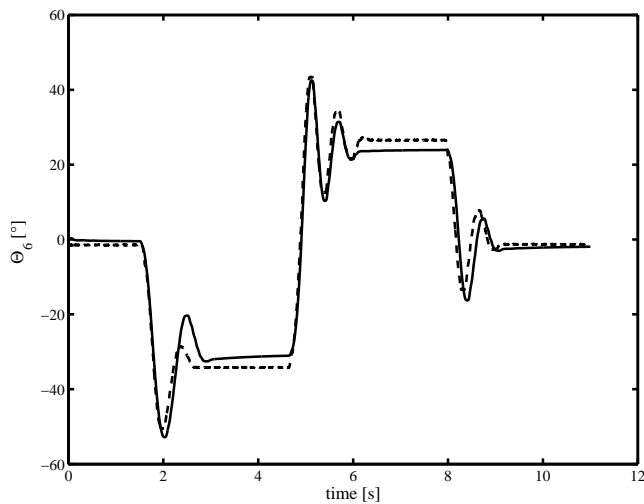
Fig. 6. Flexible arm base position

Fig. 8. Piston rod force

III-C.   Simulation results

The solution of the differential equations was implemented in MatLAB, considering as initial conditions the system at rest in a position half way the pneumatic piston stroke, and with such pressures in the actuator chambers that maintain the system at rest.

The position of the base of the flexible arm, during the evolution of the simulation is shown in figure 6, as a continuous line, and the experimental results are represented as a dashed line. The motion considered is alternative, initiated extending the cylinder rod, and considering periods at rest between movements.

The alternative motion of the mechanism, is originated by the opening and closing of the control valve, that communicates the cylinder chambers with the $0,31MPa\ abs.$ pressure supply and with the atmosphere as necessary. The
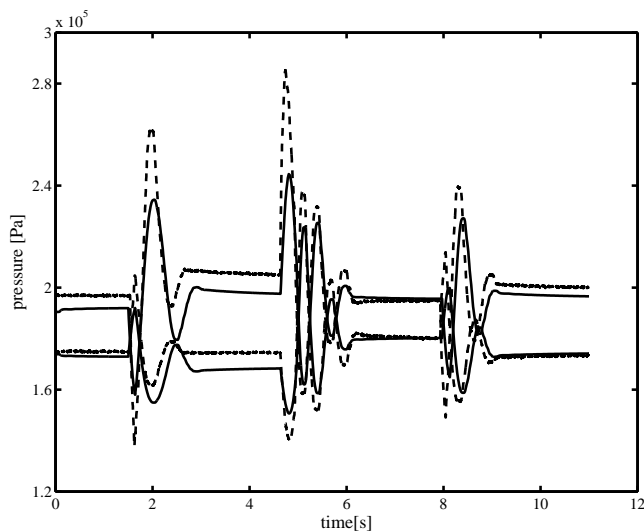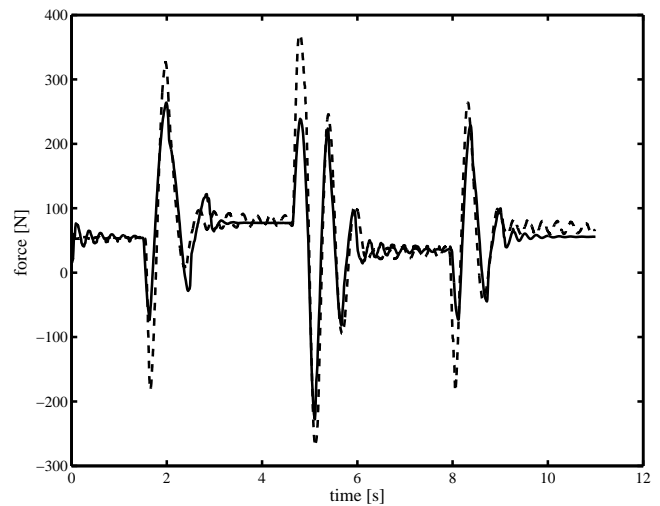
pressures calculated during the simulation for the cylinder ports, are depicted in figure 7 as continuous lines, and the experimental data as dashed lines.

The actuator output, is the force that moves the manipulator arm by means of the driving mechanism, the shape of this force will have a direct effect, in the vibration response of the flexible arm. The piston rod force obtained in the simulation, is shown in figure 8 as a continuous line, and the experimental data as a dashed line.

The flexible arm free end vibration, was approximated using four assumed modes, and its simulation results are shown in figure 9 as a continuous line, the dashed line represents the curve obtained from the strain gage measurements.
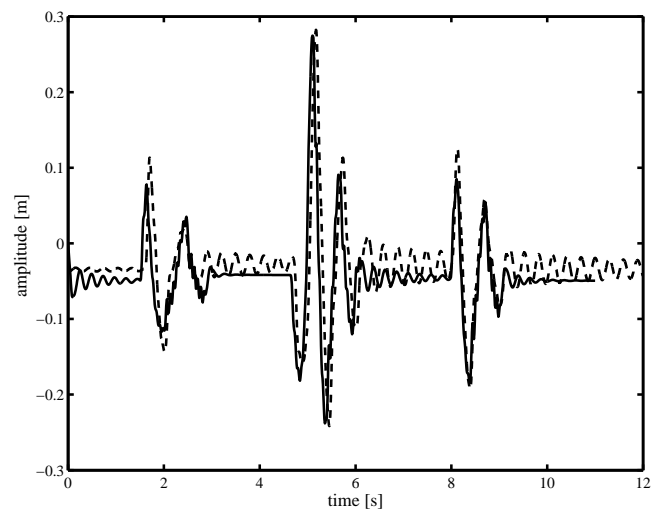

Fig. 7. Cylinder ports pressure

Fig. 9. Flexible arm free end vibration

IV. CONCLUSION

The system variables chosen to be monitored, were those considered to be more significant to the model performance. The arm base position gives at first glance, a good understanding of the manipulator intended movement. The cylinder pressures provides, the necessary energy to produce the motion. The actuator force is the intermediate variable, between the cylinder thermodynamic model and the flexible arm mechanical model. And the flexible arm free end vibration is the output variable.

For the purpose of this work, it is important to have in hand experimental data to compare the simulation results, and provide some guidelines to improve the modelling.

REFERENCES

[1] W. J. Book, *Recursive Lagrangian Dynamics of Flexible Manipulator Arms*, International Journal of Robotics Research, Vol. 3, No 3, 1984.

[2] H. Baruh and S. S. K. Tadikonda, *Issues in the Dynamics and Control of Flexible Robot Manipulators*, Journal of Guidance, Control, and Dynamics 12, No 5, 1989, pp 659-671.

[3] W. J. Book and K. Obergfell *Practical Models for Practical Flexible Arms*, Proceeding of the 2000 IEEE International Conference on Robotics & Automatition, 2000.

[4] P. B. Usoro, R.Ñadira and S. S. Mahil, *A Finite Element/Lagrange Approach to Modeling Lightweight Flexible Manipulators*, Journal of Dynamic Systems, Measurement and Control, Vol. 108, Sept. 1986, pp. 198-205.

[5] M. O. Tokhi, Z. Mohamed, S. H. M. Amin and R. Mamat, *DYNAMIC CHARACTERISATION OF A FLEXIBLE MANIPULATOR SYSTEM THEORY AND EXPERIMENTS*, TENCON 2000. Proceedings, Volume: 3, Sept. 2000, pp. 167-172.

[6] T. Yoshikawa and K. Hosoda, *Modeling of flexible Manipulators Using Virtual Rigid Links and Passive Joints*, IEEE/RSJ International Workshop on Intelligent Robots and Systems, Nov. 1991, pp. 967-972.

[7] J. J. Feliu, V. Feliu and K. C. Cerrada, *Load Adaptive Control of Single-Link Flexible Arms Based on a New Modeling Technique*, IEEE Transactions on Robotics and Automation, Vol. 15, No 5,Oct. 1999, pp. 793-804.

[8] E. Vargas, G. Reynoso, L. Villareal and R. Mier, *Diseño de un robot industrial para aplicaciones de limpieza en subestaciones eléctricas*, 3er Congreso Mexicano de Robótica, Querétaro. Asociación Mexicana de Robótica,Sept. 2001.

[9] H. Baruh and V. Radisavljevic, *MODELING OF CLOSED KINEMATIC CHAINS WITH FLEXIBLE LINKS*, Department of Mechanical and Aerospace Engineering, Rutgers University.

[10] H. Baruh, *Analytical Dynamics*, WCB McGraw-Hill, 1999.

[11] E. Hairer and G. Wanner, *Solving Ordinary Differential Ecuations II*, 2nd ed. Springer-Verlag, 1996.

[12] J. Wang, D. J. D. Wang, P. R. Moore and J. Pu, *Modelling study, analysis and robust servocontrol of pneumatic cylinder actuator systems*, IEE Proc.-Control Theory Appl., Vol. 148, No. 1, January 2001, pp. 35-42.

[13] J. M. Tressler, T. Clement, H. Kazerooni and M. Lim, *Dynamic Behavior of Pneumatic Systems for Lower Extremity Extenders*, Proc. of the 2002 IEEE Int. Conf. on Robotics & Automation, Washington, DC, May 2002, pp 3248-3253.

[14] F. Kiyama and E. Vargas, *Modelo integral del accionamiento neumático para un robot flexible industrial*, 2° Congreso Nacional de Mecatrónica, México, D.F. Universidad Anahuac del Sur, Asociación Mexicana de Mecatrónica A.C. November 2003, pp 70-77.

[15] B. L. Van de Vrande, D. H. Van Campen and A. De Kraker, *Some aspects of the analysis of stick-slip vibrations with an aplication to drillstrings*, Proceedings of ASME Design Engineering Technical Conference, 1997.

[16] R. L. Norton, *Design of Machinery*, 2nd ed. McGraw-Hill, 1999.